

## Enhanced Arsenic(V) Removal from Aqueous Solution by a Novel Magnetic Biochar Derived from Dairy Cattle Manure

Zuhal Akyürek<sup>\*,†</sup>, Hande Çelebi<sup>\*\*</sup>, Gaye Ö. Çakal<sup>\*\*\*</sup> and Sevnur Turgut<sup>\*\*\*\*</sup>

*\*Burdur Mehmet Akif Ersoy University, Faculty of Engineering and Architecture,  
Department of Energy Systems Engineering, Istiklal Campus, Burdur, Turkey*

*\*\*Eskişehir Technical University, Faculty of Engineering, Department of Chemical Engineering, İki Eylül Campus, Eskişehir, Turkey*

*\*\*\*Ankara University, Institute of Nuclear Sciences, Beşevler 10. Yıl Campus, Ankara, Turkey*

*\*\*\*\*Burdur Mehmet Akif Ersoy University, Graduate School of Natural Sciences,  
Department of Material Sciences Engineering, Istiklal Campus, Burdur, Turkey*

(Received 30 December 2021; Received in revised form 7 March 2022; Accepted 23 March 2022)

**Abstract** – Magnetic biochar produced from pyrolysis of dairy cattle manure was used to develop an effective sorbent for arsenic purification from aqueous solution. Biomass and magnetized biomass were pyrolyzed in a tube furnace with 10 °C/min heating rate at 450 °C under nitrogen flow of 100 cm<sup>3</sup>/min for 2 h. Biochars were characterized by SEM-EDX, BET, XDR, FTIR, TGA, zeta potential analysis. The resultant biochar and magnetic biochar were opposed to 50-100-500 ppm As(V) laden aqueous solution. Adsorption experiments were performed by using ASTM 4646-03 batch method. The effects of concentration, pH, temperature and stirring rate on adsorption were evaluated. As(V) was successfully removed from aqueous solution by magnetic biochar due to its highly porous structure, high aromaticity and polarity. The results suggest dairy cattle manure pyrolysis is a promising route for managing animal manure and producing a cost effective biosorbent for efficient immobilization of arsenic in aqueous solutions.

Key words: Arsenic, Dairy cattle manure, Magnetic biochar, Adsorption, Wastewater treatment

### 1. Introduction

Progressive growth in world population and intensive industrial activity has led to contamination of surface and groundwater with heavy metals such as lead, cadmium, chromium, mercury and arsenic that threaten all forms of life. Among all the heavy metals, arsenic (As) has the most severe adverse effects on human health through drinking water contamination [1]. It is a carcinogenic element that can be transferred to water sources naturally (weathering, erosion, volcanic activity) or by anthropogenic activities such as mining, petroleum refining, fertilizer, chemicals, power and other manufacturing industries [2]. In addition, anthropogenic arsenic contamination by discharge and disposal of As-containing compounds may lead to even greater arsenic concentrations [3-5].

Arsenic naturally occurs in the environment in two inorganic forms, arsenite (H<sub>3</sub>AsO<sub>3</sub>, H<sub>2</sub>AsO<sub>3</sub>) and arsenate (H<sub>2</sub>AsO<sub>4</sub> and HAsO<sub>4</sub>), as a result of its natural geological presence in soils, sediments and ground and surface water systems [6-8]. Because of the severe toxicity impacts of arsenic on humans, the maximum allowance limit of 10 µg/L in drinking water was prescribed by the World Health Organization (WHO). Arsenic concentration in contaminated water and wastewater changes in the range of 0.1–230 mg/L, which is

much greater than the maximum allowable limit [9]. Therefore, there is serious need for removing arsenic from drinking water and wastewater. The most common techniques used for arsenic removal from aqueous solutions are precipitation [10], coagulation [11], membrane separation [12], ion exchange [13], reverse osmosis [14] and sorption [15]. Among these, sorption is considered to be the most effective method for heavy metal remediation in waste water [16]. This is mainly due to its ease in operation, low-cost and highly efficient process with small footprint [17].

Several sorbents have been developed for adsorption of heavy metals such as synthetic zeolites and alumina or iron modified zeolites [17,18], commercial activated carbon [19], iron oxides [20] from contaminated aqueous medium. High cost, instability and regeneration problems have impeded the use of these sorbents [8]. Hence, the research focus has been diverted to more environmentally friendly, low cost and high performance sorbents to remove arsenic from aqueous solutions. Biochar is a high carbon content pyrogenic solid material obtained by thermal degradation of biomass in an oxygen-free medium. Biochars have the potential to act as surface sorbents or in other terms bio-sorbents like activated carbon, due to their highly porous carbon matrix and large surface area with oxygen functional groups, and thus play an important role in the control of environmental pollutants [21-22]. In this respect, biochar produced as a result of biomass pyrolysis has gained importance as a cheap and effective surface sorbent.

Sorption capacity of biosorbents depends mainly on biomass characteristics and operational process parameters that enhance the

<sup>†</sup>To whom correspondence should be addressed.

E-mail: drzuhalakyurek@gmail.com; zuhalakyurek@mehmetakif.edu.tr  
This is an Open-Access article distributed under the terms of the Creative Commons Attribution Non-Commercial License (<http://creativecommons.org/licenses/by-nc/3.0>) which permits unrestricted non-commercial use, distribution, and reproduction in any medium, provided the original work is properly cited.

surface area, porosity and occurrence of functional groups. For instance, even if the surface area of biochar increases with increasing the pyrolysis temperature, optimization of the pyrolysis process is necessary as high temperatures can lead to the destruction of functional groups [23]. Vast literature on biochar adsorption of different metals, such as Pb, Cu, Zn, Cd, Cr, and Hg, is available [24-27]. However, studies on As removal from aqueous solutions are less conducted. Recent studies have confirmed that biochar has high pollutant sorption capacity due to its surface effective functional groups [28]. Agrafioti et al. [29] stated that approximately 40% arsenic adsorption can be achieved from biochar produced from pyrolysis of rice husk, domestic waste and sewage wastes. Wang et al. [30] obtained that biochars synthesized from the pyrolysis of wood and grass wastes at 600 °C have surface area of 209 m<sup>2</sup>/g and 182 m<sup>2</sup>/g and about 0.250 mg/g As (V) adsorption capacity. In recent years, new techniques have improved biochar by modifications to enhance the sorption capacity to contaminants. Adsorption capacity of biochar can be enhanced by modifications to increase the surface area for adsorption and the amount of the functional groups. Aluminum [31], manganese [32], iron oxide [33] based reagents have been used to improve the adsorption capacity and magnetic ability of different biochar sorbents. Especially, iron oxides have shown high affinity and selectivity in arsenic sorption [34]. Hence, in order to improve the arsenic adsorption capacity, research has been focused on iron oxide modified biochar. Wang et al. [35] prepared iron oxide modified biochar from pine tree biomass and natural hematite. Pyrolysis at 600 °C results in 209 m<sup>2</sup>/g surface area and 1.6 times more As(V) adsorption capacity with respect to untreated biochar. Zhang et al. [36] stated that As(V) adsorption capacity of biochar produced from pyrolysis of FeCl<sub>3</sub>-treated cotton stalk was comparable with commercial adsorbents. According to Agrafioti et al. [29], Ca and Fe modified rice husk has shown over 95% As(V) removal performance.

Turkey has huge biomass potential of 8.6 million tons of oil equivalent (MTOE) generated by agricultural, animal and urban wastes. Animal manure energy potential in Turkey is equivalent to about 1.3 MTOE/year [37]. In recent years, valorization of these organic wastes has become clearly necessary in order to meet the growing energy needs, to reduce the dependency on imported energy, to increase the use of renewable resources against climate change and to ensure sustainable development. Agricultural and animal wastes are usually used as fuel or disposed of on the fields. Utilization of these waste materials with sustainable conversion technologies has multiple advantages in terms of environmental and human health protection by reducing waste volume and in terms of economy by producing useful energy and high value added green chemicals. To the best of the authors' knowledge, no study has been published about As(V) adsorption from aqueous solutions by biochar and magnetic biochar derived from dairy cattle manure. In this study, in order to convert animal waste into valuable green adsorbents, iron modified biochar was produced from pyrolysis of dairy cattle manure, aiming at the enhancement of As(V) adsorption ability of biochar. Effect of

concentration, pH, and temperature on the As(V) was evaluated together with sorption isotherm.

## 2. Materials and Methods

### 2-1. Materials

All chemicals used in this study were analytical grade and dissolved in deionized water (18.2 M °C). Sodium arsenate dibasic heptahydrate (Na<sub>2</sub>HAsO<sub>4</sub>·7H<sub>2</sub>O) and ferric chloride hexahydrate (FeCl<sub>3</sub>·6H<sub>2</sub>O) were purchased from Sigma Aldrich. Cattle manure was supplied from a local farm in Ağlasun, Burdur, Turkey. The primary analyses of the cattle manure are shown in Table 1. Moisture, volatile matter, ash content of the samples was determined by ASTM D3173, ASTM D3175, ASTM D3174, respectively. The major elements (C, H, N, S) were tested by LECO CHNS-932 elemental analyzer and the content of O was calculated by the difference. Magnetization did not result in a considerable change in the elemental composition of biomass. The elemental composition of magnetic biochar is closely related to the raw material from which it derives. The mineral content of biomass was analyzed by XRF. Heating value of biomass was determined by IKA WERKE calorimeter.

### 2-2. Preparation of biochar and magnetic biochar

The manure sample was dried in oven overnight at 80 °C and then

**Table 1. Chemical analysis of dairy cow manure**

Proximate Analysis (as received, wt.%)	
Moisture	5.98
Volatile Matter	53.52
Fixed Carbon	16.24
Ash	24.26
Elemental Analysis (dry basis, wt.%)	
C	33.07
H	4.87
N	2.90
S	0.63
O	58.53
H/C molar ratio	1.77
O/C molar ratio	1.33
(O+N)/C	1.40
(O+N+S)/C molar ratio	1.41
XRF Analysis	
Na, %	0.37
Mg, %	0.42
Al, %	0.45
Si, %	3.00
P, %	0.43
Cl, %	0.22
K, %	1.46
Ca, %	5.44
Fe, %	0.45
Mn, %	0.05
LHV, MJ/kg	13.55
HHV, MJ/kg	14.86

sifted out 0.5-1 mm size. Dairy cattle manure biochar (DCM) was prepared by pyrolyzing in a tubular reactor (Proterm PTF16/75/450) with 10 °C/min heating rate under nitrogen flow of 100cm<sup>3</sup>/min at a peak temperature of 450 °C temperature for 2 h. For producing the magnetic biochar (MDCM), ferric chloride solution was prepared by dissolving 30 g of ferric chloride hexahydrate (FeCl<sub>3</sub>.6H<sub>2</sub>O, Sigma-44944) in 70 ml of DI water. 10 g of cattle manure was immersed into the prepared solution and the resulting mixture was sonicated for 2 h and then filtered on Whatman No. 42 filter paper. Then, the mixture was washed with DI water and dried in oven at 80 °C for 2 h under air atmosphere. The pretreated manure was pyrolyzed in tube furnace at a temperature of 450 °C in nitrogen environment for 2 h and sealed in a container before used.

### 2-3. Characterization

The structural property of magnetic biochar was determined by XRD Rikagu Miniflex 600 X-ray diffractometer with nickel-filtered Cu KR radiation at 30 kV and 24 mA. The powdered samples of adsorbent were scanned from 5 to 85°. The morphology of biochar surface before and after adsorption of As(V) was examined by scanning electron microscopy (Quanta 400F Field Emission SEM) equipped with energy dispersive X-ray spectroscopy. Fourier transform infrared (FTIR) spectroscopy was performed to determine the functional groups on biochar surface using a Bruker Tensor 27 FTIR-ATR spectrometer. The surface area of biochar and magnetic biochar was analyzed with nitrogen adsorption isotherms at 77 K using Autosorb-6B Surface Area and Pore Size Analyzer (Quantachrome, Instruments, USA). The samples were degassed at 100 °C for 9 h before N<sub>2</sub> adsorption. The multi-point Brunauer-Emmett-Teller (BET) method was used to calculate the total surface area. Zeta potential of biochar samples was determined by Malvern Nano ZS90. Thermal stability of biochar samples was examined by thermogravimetric analysis (TGA) (Seiko SII TG/DTA 7200, Hitachi Corp., Japan) under a nitrogen atmosphere, heated from room temperature to 1000 °C.

### 2-4. Adsorption experiments

Stock As(V) solutions of 50, 100, 500 ppm were prepared by dissolving appropriate amounts of Na<sub>2</sub>HAsO<sub>4</sub>.7H<sub>2</sub>O in de-ionized water. The pH of the solutions was manually adjusted by dropwise addition of 0.1 M HCl and 0.1 M NaOH. Adsorption experiments were performed by batch method by using ASTM 4646-03 of Standard test method for 24 h batch-type measurement of contaminant sorption by soils and sediments. 0.5 g of biochar was weighed into a 50 ml glass bottle and 10 ml of As(V) solution was added on the biochar. The bottles were sealed and shaken at 150 rpm in an orbital incubator (Stuart S1500) at room temperature for 24 h. At appropriate times, the samples were withdrawn from the incubator and immediately filtered by Whatman No. 42 filter paper. The remaining As(V) concentration in the solution was detected by inductively coupled plasma optical emission spectroscopy (ICP-OES, Perkin Elmer, Optima

4300 DV). As(V) concentration adsorbed on biochar was calculated from initial and final aqueous concentrations as follows [38]:

$$q_e = \frac{(C_0 - C_e)V}{W} \quad (1)$$

where  $q_e$  is the equilibrium As(V) concentration (mg/g) in the solid phase,  $C_0$  and  $C_e$  (mg/L) are the initial and equilibrium concentration of As(V) in the liquid phase, respectively,  $W$  (g) is the adsorbent amount and  $V$  (L) is the volume of As(V) solution. The percentage of As(V) removal from aqueous solution by DCM and MDCM was calculated by Eq. (2) as follows:

$$\% \text{As(V) removal} = \frac{(C_0 - C_e)}{C_0} \times 100 \quad (2)$$

### 2-5. Adsorption isotherm

Sorption isotherms were fitted to the Langmuir (Eq. 3) and Freundlich (Eq. 4) equations to quantify the adsorption capacity of DCM and MDCM. The models are described as follows [38]:

$$\text{Langmuir: } q_e = \frac{q_{\max} b C_e}{(1 + b C_e)} \quad (3)$$

$$\text{Freundlich: } q_e = K C_e^{1/n} \quad (4)$$

where  $q_e$  (mg/g) is the amount of metal adsorbed per unit weight of adsorbent,  $C_e$  (mg/L) is the equilibrium solution concentration of adsorbate,  $q_{\max}$  (mg/g) is the maximum amount of adsorbed metal ions to form monolayer on surface of adsorbent,  $b$  (L/mg) is the Langmuir adsorption constant and  $K$  (( $\mu\text{g/g}$ )(L/ $\mu\text{g}$ )<sup>1/n</sup>) is the Freundlich adsorption constant and  $(1/n)$  is constant for the strength of adsorption [39].

## 3. Results and Discussion

### 3-1. Characterization of DCM and MDCM

Physicochemical properties of biochar have great influence on heavy metal sorption capacity. Hence, characterization of biochar prior to adsorption process such as surface area, porosity, zeta potential, functional groups is necessary. Surface area and porosity of biochar, which generally depend on pyrolysis operating conditions, are important factors changing the metal sorption capacity of biochar. Higher pyrolysis temperature (> 600-700 °C) leads to larger pore size for metal sorption; however, it may also result in reduced surface area due to possible structural destruction [40]. Biomass properties have also affected pore size of biochar. Lignin-rich biomass is generally known to have macro-pore size, whereas cellulose rich biomass has micro-porous crystal structure [41]. High lignocellulose concentration is found in animal manure, as animals are fed with plants such as grass, straw, etc. Dairy cattle manure is known to have lignin content of ~18.0 % [42]. Biochar produced at lower pyrolysis temperatures contains more functional groups (C=O, C-H) to remove the contaminants. (H/C) and (O/C) molar ratios are generally used as

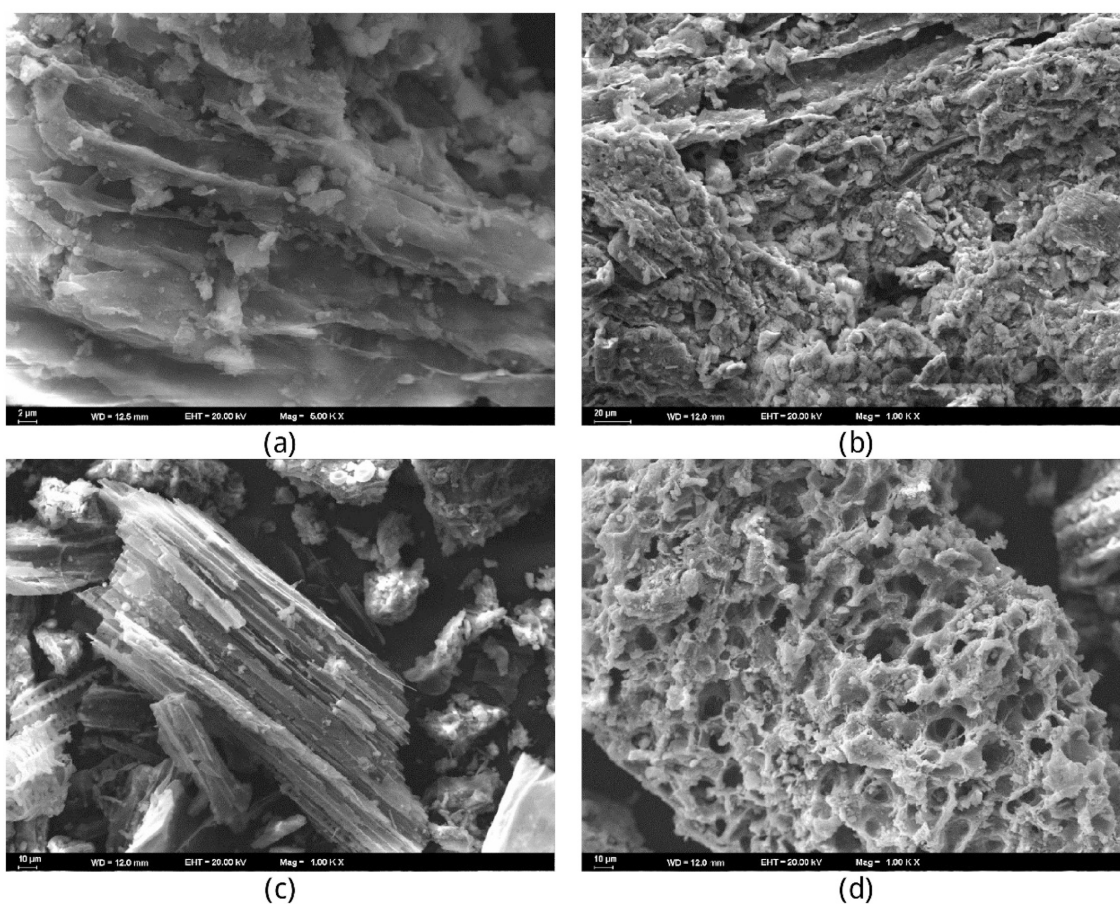
**Table 2. Chemical analysis of DCM**

	DCM
C %	29.13
H %	2.37
N %	2.92
S %	0.33
O %	65.25
H/C molar ratio	0.98
O/C molar ratio	1.68
(O+N)/C molar ratio	1.77
(O+N+S)/C molar ratio	1.77
Na, %	0.200
Mg, %	0.185
Al, %	0.135
Si, %	1.484
P, %	0.253
Cl, %	0.060
K, %	0.532
Ca, %	1.946
Fe, %	0.185
Mn, %	0.019

indicators of aromaticity and surface hydrophilicity, respectively, and the molar ratio of [(O+N)/C] and [(O+N+S)/C] is used for estimation of

polarity of the functional groups [38]. DMC has shown to have high aromaticity and polarity. In biochar production, lower operating temperature of 450 °C has been selected in order to have higher biochar yield and surface functional groups. Biochar yields of biomass and magnetic biomass were obtained as 54% and 73%, respectively. Table 2 shows the chemical analysis results for dairy cattle manure derived biochar (DCM).

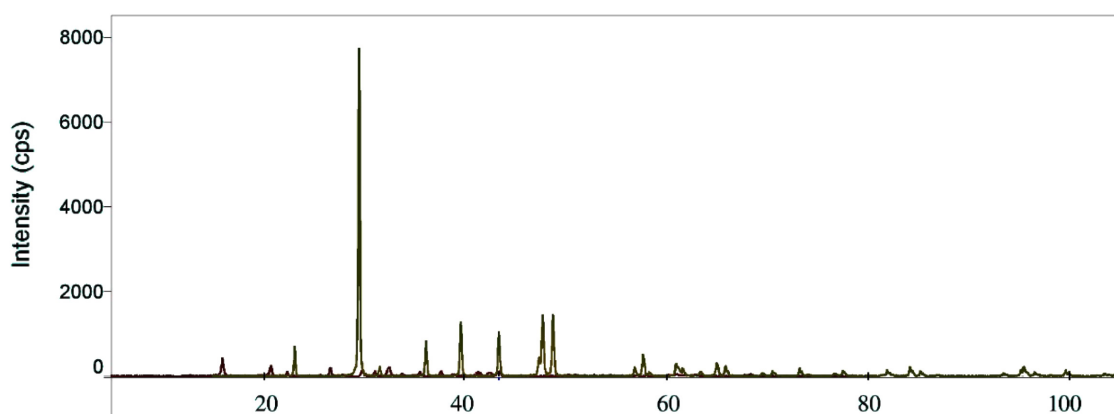
Surface area of mesoporous structure in biochar was detected as 10.78 m<sup>2</sup>/g, whereas surface area of magnetic biochar was 21.35 m<sup>2</sup>/g. The surface morphology of biochar before and after As(V) adsorption was examined by SEM (Fig. 1). As can be clearly seen from the figure, MDCM has shown to have extremely porous structure compared to DCM. Occurrence of additional microporous structure in magnetic biochar supported enhanced adsorption capacity. DCM crystal structure (Fig. 1(a)) was observed to be in the form of platelet crystallites, whereas MDCM crystal structure (Fig. 1(b)) was formed by spherical crystal agglomerates in cage structure. The analysis showed that Fe<sub>3</sub>O<sub>4</sub> was uniformly deposited and impregnated on biochar matrix, which is an indicative of strong mechanical bonding [8]. EDX analysis given in Table 3 has shown the presence of high amounts of Fe and O elements in MDCM. The presence of C and O also implies the oxygen containing surface functional groups which have great influence on promoting the adsorption ability of biochar. The



**Fig. 1.** SEM images of biochar (a) before adsorption, DCM, (b) before adsorption, MDCM, (c) after As(V) adsorption on DCM, (d) after As(V) adsorption on MDCM.

**Table 3. EDX Analysis results**

Elements	DCM before adsorption	MDCM before adsorption	DCM after adsorption	MDCM after adsorption
O, wt.%	43.67	19.91	51.21	31.37
C, wt.%	40.69	2.02	36.52	9.17
Si, wt.%	1.50	6.04	5.51	1.15
Fe, wt.%	-	34.85	-	45.66
Cl, wt.%	-	30.57	-	4.52
As, wt.%	-	-	1.26	2.90
P, wt.%	3.29	2.13	1.69	2.21
K, wt.%	2.87	0.32	0.60	0.04
S, wt.%	1.17	0.83	0.60	0.59
Ca, wt.%	3.27	2.53	2.42	0.78

**Fig. 2. XRD pattern of MDCM.**

carbon amount was seen to reduce in magnetic biochar, which is in correspondence with elemental analysis results. After adsorption (Fig. 1(c), (d)) arsenic was detected in biochar crystal structure. MDCM has shown to adsorb higher amount of As(V) compared to DCM.

X-ray spectroscopy for MDCM presented in Fig. 2 shows that magnetic biochar has highly crystalline structure which supports the results of SEM analyses. Iron in biochar structure is indicated by characteristic peaks of maghemite ( $\gamma\text{-Fe}_2\text{O}_3$ ) ( $2\theta = 35.5^\circ$  and  $63.0^\circ$ ) and hematite ( $\alpha\text{-Fe}_2\text{O}_3$ ) ( $2\theta = 33.15^\circ$  and  $40.85^\circ$ ) (PDF33-0664) [8]. The reducing atmosphere during pyrolysis led to reduction of maghemite to magnetite ( $\text{Fe}_3\text{O}_4$ ) [33]. The major peaks of magnetite ( $\text{Fe}_3\text{O}_4$ )  $2\theta = 30, 35.4, 43, 57.4, 62.8, 75^\circ$  [43] reveal presence of Fe in biochar structure.

Surface functional groups of DCM and MDCM were analyzed before adsorption by FTIR spectroscopy. FTIR spectra of biochar and magnetic biochar are depicted in Fig. 3. The FTIR spectra were focused on wavenumber interval of  $500\text{--}4000\text{ cm}^{-1}$ . There are various peaks in the spectra representing the functional groups in DCM and MDCM. Four peaks are found at wavenumbers of  $1553, 1304, 1071,$  and  $873\text{ cm}^{-1}$ , respectively, which are ascribed to the vibration of the C=C, O=C-O, C-O and aromatic C-H [29]. The band at  $\sim 1712\text{ cm}^{-1}$  and  $2354\text{ cm}^{-1}$  corresponds to vibration of C=O and C-H bonds, respectively. The peaks at  $3800\text{--}3100\text{ cm}^{-1}$  are due to stretching vibration of -OH [8,44]. The FTIR spectrum of MDCM shows that

there is a broader band at around  $700\text{--}660\text{ cm}^{-1}$  due to maghemite ( $\gamma\text{-Fe}_2\text{O}_3$ ) in biochar [45]. Iron impregnation has shown to enhance the oxygen containing surface functional groups. The peaks at  $1013$  and  $1598\text{ cm}^{-1}$  represent C-O, C=O and Fe-O, Fe-OH bonding. The characteristic bands of hydroxyl groups ( $3000\text{--}3650\text{ cm}^{-1}$ ) are also seen in the FTIR spectrum of MDCM. FTIR spectra of biochar after adsorption show peaks in the range of  $650\text{--}950\text{ cm}^{-1}$  which are indicative of As-O bonding. Peak with wavenumber  $2930\text{ cm}^{-1}$  present on DCM biochar surface disappeared after adsorbing As(V). The slight changes in intensities of peaks after adsorption might be responsible for the deposition of As(V) on the surface of biochar.

Thermal behavior of biomass and magnetic biomass was examined by TGA. Comparison of the DTG curves (Fig. 4) shows that MDCM is decomposed in two steps, whereas DCM is known to have degradation in three steps [46]. The residual amount was found to be higher in MDCM (34%) than DCM (30%). MDCM structure is thermally more stable than DCM and hence degradation has shifted to higher temperatures. This can be attributed to thermally inactive chemical bonding of iron oxide and surface functional groups, which is in agreement with previous studies [35]. All the analysis results given above have supported the successful synthesis of magnetic biochar.

### 3-2. Adsorption of As(V) from aqueous solution

In order to have a sustainable water treatment methodology it is important to consider the effect of different parameters on adsorption.

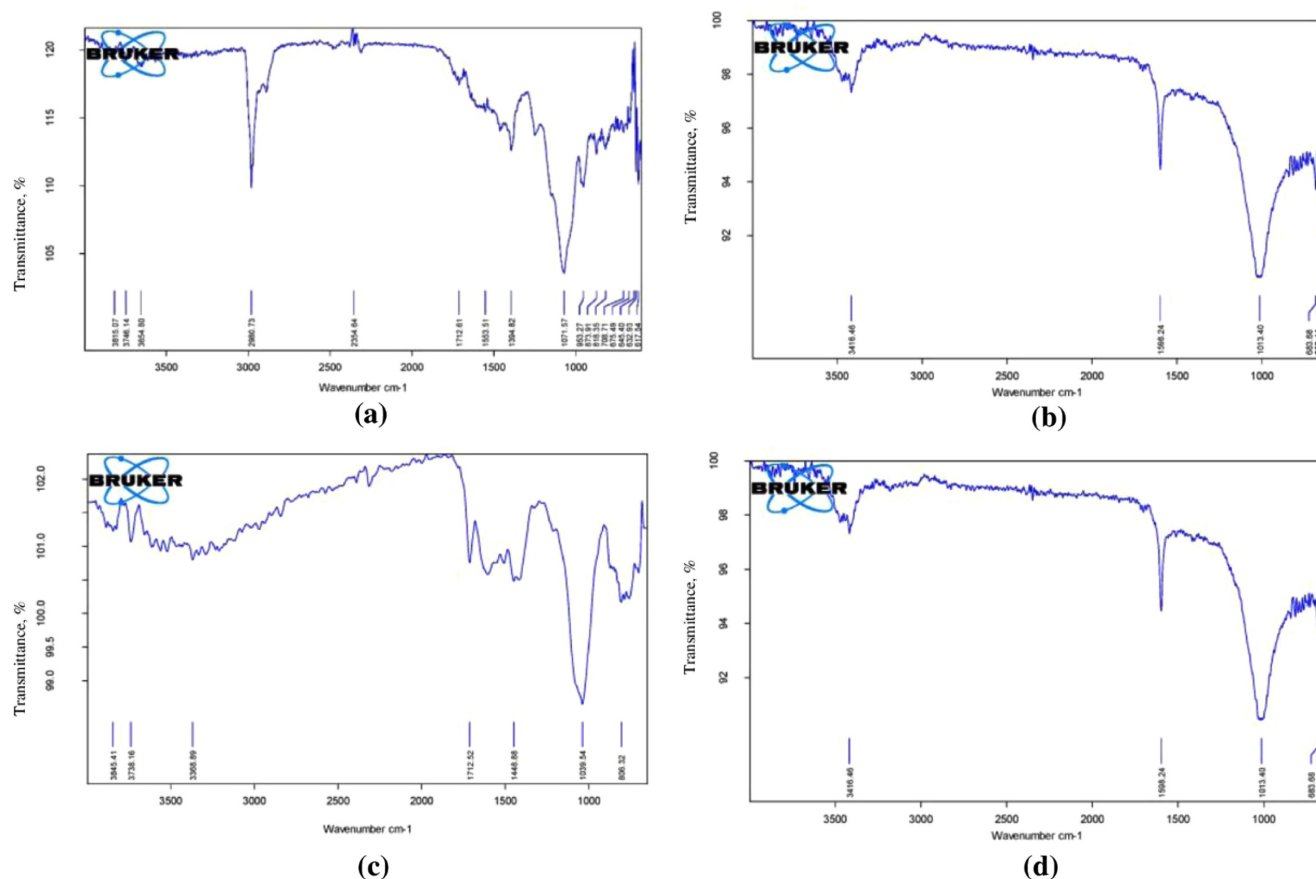


Fig. 3. FTIR Spectra of (a) before adsorption, DCM, (b) before adsorption, MDCM, (c) after As(V) adsorption, DCM, (d) after As(V) adsorption, MDCM.

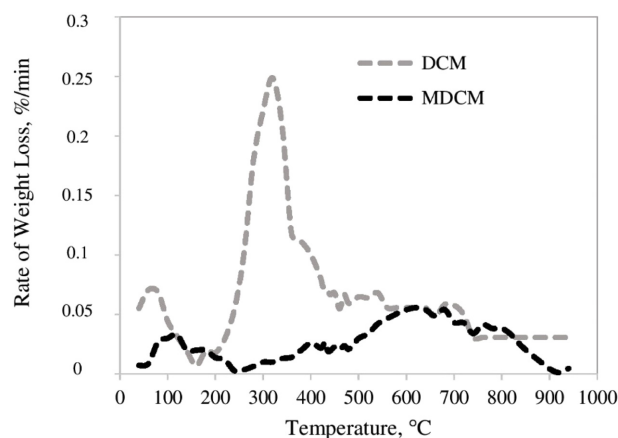


Fig. 4. DTG curves of DCM and MDCM.

In this study, As(V) removal efficiency of biochar and magnetic biochar prepared from pyrolysis of animal manure was investigated by batch type adsorption as functions of initial As(V) concentration, pH, temperature and stirring rate.

### 3-2-1. Effect of Initial As(V) Concentration

Figure 5 presents the effect of initial As(V) concentration, which was selected as 50, 100 and 500 mg/L, for arsenic removal carried

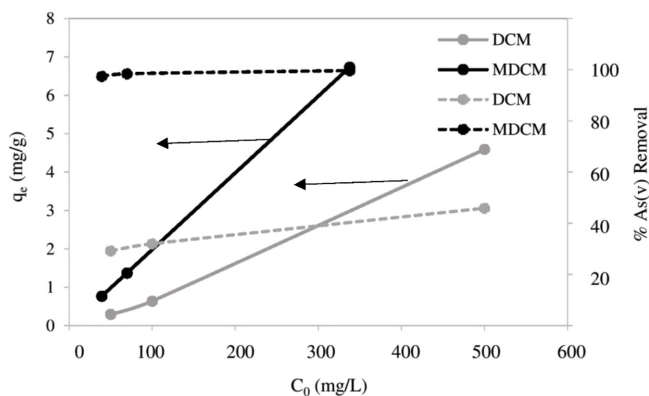


Fig. 5. Effect of initial As(V) concentration.

out at pH 7 for adsorption period of 24 hours at room temperature. As can be seen from the figure, an increase in initial concentration increased the removal efficiency of DCM from 29.2% to 45.9%. Magnetic biochar, MDCM, on the other hand conducted a rapid and 100% As(V) uptake in the initial concentration range of 50-500 mg/L. High As(V) removal efficiency for magnetic biochar is in agreement with previous studies [29,36]. The impact of other parameters was studied at 500 mg/L initial As(V) concentration to reach higher As(V) removal rate.

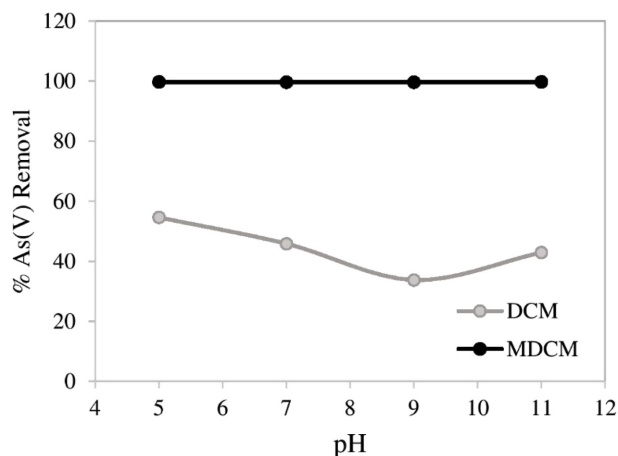


Fig. 6. Effect of pH on As(V) removal.

### 3-2-2. Effect of pH

The pH of an aqueous solution strongly affects As(V) adsorption because it influences the surface charge of biochar and the speciation of As(V) in aqueous solutions. The effect of solution pH on As(V) adsorption on DCM and MDCM was examined in the range of 5-11 (Fig. 6). The highest removal efficiency was at pH = 5 for DCM and was reduced from 54.7% to 33.8% at pH = 9. Iron impregnation resulted in greater sorption capacity. For magnetic biochar, MDCM, 100% removal efficiency was achieved irrespective of pH value. The form of arsenic species in aqueous media changes according to solution pH. For instance, when pH is smaller than 2.5,  $H_3AsO_4$  dominates, when pH is changing in between 2.5 and 7,  $H_2AsO_4^-$  prevails, and when pH is greater than 7, the dominant form is  $HASO_4^{2-}$ . It is reported that when biochars are negatively charged, electrostatic repulsive forces can limit their adsorption capacity for arsenate [47]. Zeta potential of DCM and MDCM was measured as -13.6 mV and 27.4 mV, respectively, supporting higher adsorption of As(V) on MDCM. At high pH values, the presence of excess  $OH^-$  groups competed with anionic functional groups and lowered removal rate of As(V) from aqueous solution [48].

### 3-2-3. Effect of Temperature

Adsorption temperature is known to have strong influence on removal of species. The effect of adsorption temperature on As(V) uptake was investigated at four different adsorption temperatures of 22 °C, 40 °C, 60 °C and 80 °C. The maximum adsorption capacity was obtained at 80 °C with initial As(V) concentration of 500 mg/L. Fig. 7 shows that increase in adsorption temperature enhanced the As(V) removal of DCM from 45.9% to 99.74%. MDCM was shown to have 100% As(V) removal irrespective of temperature change. The incremental change in adsorption capacity with increasing temperature predicted that the adsorption process of As(V) adsorption on DCM was endothermic.

### 3-2-4. Effect of stirring rate

In order to investigate the effect of stirring rate, adsorption of

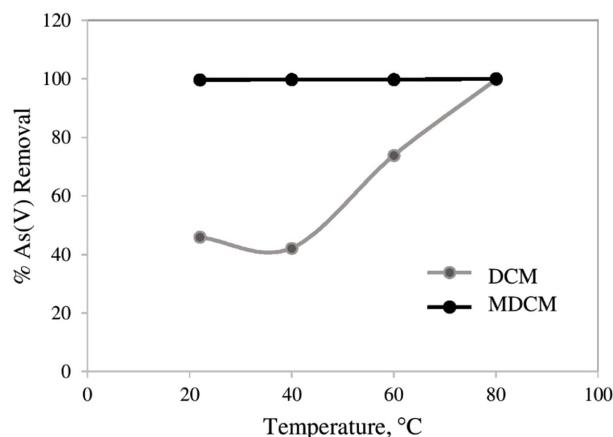


Fig. 7. Effect of adsorption temperature on As(V) removal.

Table 4. The parameters of isotherms of As(V) sorption by DCM and MDCM

Sorbent	Langmuir	Freundlich
DCM	$q_{max} = 2.48 \text{ mg/g}$ $K = 3.523 \times 10^{-3} \text{ L/mg}$ $R^2 = 0.99$	$K = 2.56 \times 10^{-4} \text{ mg}^{(1-n)} \text{ L}^n \text{ kg}^{-1}$ $n = 0.519$ $R^2 = 0.89$
MDCM	$q_{max} = 5.30 \text{ mg/g}$ $K = 2.934 \text{ L/mg}$ $R^2 = 0.98$	$K = 12.36 \text{ mg}^{(1-n)} \text{ L}^n \text{ kg}^{-1}$ $n = 1.733$ $R^2 = 0.94$

As(V) on DCM and MDCM was carried out in stagnant conditions. The results revealed that stirring of the solution did not have a significant impact on adsorption capacity of biochar. As(V) removal was shown to increase from 39.5% to 45.9% during adsorption by DCM, while the removal rate stayed constant at maximum irrespective of the stirring rate during As(V) adsorption on MDCM.

### 3-3. Adsorption Isotherm

Langmuir and Freundlich isotherm models were used to describe the adsorption of As(V) on biochar and magnetic biochar. The estimated model parameters are presented in Table 4. Maximum adsorption capacity increased from 2.48 mg/g to 5.30 mg/g with iron impregnation. These findings reveal that iron impregnation enhanced the sorption affinity of biochar for As(V) [49] more than two times. In comparison, the maximum As(V) adsorption capacity of MDCM was found to be higher than a range of iron based sorbents (Table 5).

### 3-4. Recyclability of MDCM

The reusability potential of biochar contributes to the economic importance of the biosorption process. In this study, NaOH was used as the desorbing agent. During regeneration, acid digestion may result in iron loss in biochar, hence basic NaOH is considered as an effective desorbing agent for As(V) removal from magnetic biochar [49,54]. For desorption study of As(V) loaded biochar, 0.5 M NaOH was used by keeping the other operating conditions the same as for adsorption. Three cycles of desorption and resorption experiments were performed. 0.5 M NaOH was able to desorb 73% of initially

**Table 5. Comparison of As(V) sorption capacity of different adsorbents**

Sorbent	pH of mixture	Initial As(V) concentration (ppm)	q <sub>max</sub> (mg/g)	Reference
Iron hydroxide activated carbon	6-8	< 1	1.25	[50]
Fe-impregnated granular activated carbon	7	40	1.95	[51]
Fe(III)-coated rice husk	4	5	2.50	[52]
Cottonwood derived biochar/ $\gamma$ -Fe <sub>2</sub> O <sub>3</sub> composite	-	5-200	3.147	[36]
Magnetic Kans grass derived biochar	7	0-0.8	3.13	[43]
Magnetic walnut shell derived biochar	7	0.1-5	1.91	[53]
Dairy cattle manure derived magnetic biochar	7	50-500	5.30	This study

sorbed As(V) on MDCM. Regeneration rate decreased from 73% to 52% in the third cycle. Similar findings have also been presented in previous studies [49]. Reduction in desorption efficiency is attributed to the loss of adsorption sites on biochar during recycling [55,56]. Considerable As(V) adsorption efficiency of magnetic biochar from aqueous solution after three regeneration cycles demonstrates the significant potential of magnetic biochar for real treatment applications.

#### 4. Conclusion

Arsenic is one of the most harmful pollutants in the environment that threatens human health. Dairy manure is a problematic waste having adverse effects on environmental and public health, triggering atmospheric pollution if not managed well. Pyrolysis is an effective thermal conversion technology for utilization of waste and converting it into useful energy and high value added, cost effective products. In this study, biochar and a novel magnetic biochar (MDCM) derived from dairy cattle manure were used for As(V) removal from aqueous solution. Compared to pristine biochar, magnetic biochar exhibited higher As(V) removal efficiency. Almost 100 % of As(V) uptake was achieved from 50, 100, 500 ppm initial solution concentrations. The removal efficiency of DCM increased by increasing initial As(V) concentration, adsorption temperature and stirring rate and reduced by increasing the solution pH. Adsorption efficiency of MDCM was obtained to be independent of all parameters. MDCM biochar has high potential to sequester As(V) concentrations from aqueous solutions.

#### Acknowledgments

Financial support provided by Burdur Mehmet Akif Ersoy University through a research project BAP-0579-YL-19 in aid of this research is gratefully acknowledged.

#### References

- Lata, S. and Samadder, S. R., "Removal of Arsenic from Water Using Nano Adsorbents and Challenges: A Review," *J. Environmental Management*, **166**, 387-406(2016).
- Viraraghavan, T., Subramanian, K. S. and Aruldoss, J. A., "Arsenic in Drinking Water Problems and Solutions," *Water Sci. Technol.*, **40**, 69-76(1999).
- Singh, R., Singh, S., Parihar, P., Singh, V. P. and Prasad, S. M., "Arsenic Contamination, Consequences and Remediation Techniques: A Review," *Ecotox. Environ. Safe.*, **112**, 247-270(2015).
- Mandal, B. K. and Suzuki, K. T., "Arsenic Around The World: A Review," *Talanta*, **58**, 201-235(2002).
- Xue, Q., Ran, Y., Tan, Y., Peacock, C. L. and Du, H., "Arsenite and Arsenate Binding to Ferrihydrite Organo-mineral Coprecipitate: Implications for Arsenic Mobility and Fate in Natural Environments," *Chemosphere*, **224**, 103-110(2019).
- Garelick, H., Jones, H., Dybowska, A. and Valsami-Jones, E., "Arsenic Pollution Sources," *Rev. Environ. Contam. Toxicol.*, **197**, 17-60(2008).
- Smith, E., Naidu, R. and Alston, A., Chemistry of Inorganic Arsenic in Soils," *J. Environ. Qual.*, **31**, 557-563(2002).
- He, R., Peng, Z., Lyu, H., Huang, H., Nan, Q. and Tang, J., "Synthesis and Characterization of An Iron-Impregnated Biochar for Aqueous Arsenic Removal," *Sci. Total Environ.*, **612**, 1177-1186 (2018).
- Matschullat, J., "Arsenic in the Geosphere - A Review," *Sci. Total Environ.*, **249**, 297-312(2000).
- Jia, Y., Xu, L., Fang, Z. and Demopoulos, G. P., "Observation of Surface Precipitation of Arsenate on Ferrihydrite," *Environ. Sci. Technol.*, **40**(10), 3248-3253(2006).
- Leupin, O. X. and Hug, S. J., "Oxidation and Removal of Arsenic (III) from Aerated Groundwater by Filtration through Sand and Zero-valent Iron," *Water Res.*, **39**(9), 1729-1740(2005).
- Kim, J. and Benjamin, M. M., "Modeling a Novel Ion Exchange Process for Arsenic and Nitrate Removal," *Water Res.*, **38**(8), 2053-2062(2004).
- Mukherjee, A., Zimmerman, A. R. and Harris, W., "Surface Chemistry Variations among A Series of Laboratory-Produced Biochars," *Geoderma*, **163**, 247-255(2011).
- Gholami, M. M., Mokhtari, M. A., Aameri, A. and Fard, M. R. A., "Application of Reverse Osmosis Technology for Arsenic Removal from Drinking Water," *Desalination*, **200**, 725-727(2006).
- Marques Neto, J. D. O., Bellato, C. R., Milagres, J. L., Pessoa, K. D. and Alvarenga, E. S. D., "Preparation and Evaluation of Chitosan Beads Immobilized with Iron (III) for the Removal of As (III) and As (V) from Water," *J. Braz. Chem. Soc.*, **24**(1), 121-132(2013).
- Lin, L., Qui, W., Wang, D., Huang, Q., Song, Z. and Chaud, H. W., "Arsenic Removal in Aqueous Solution by a Novel Fe-Mn Modified Biochar Composite: Characterization and Mechanism," *Ecotoxicology and Environmental Safety*, **144**, 514-21(2017).
- Qiu, W. and Zheng, Y., "Arsenate Removal from Water by An

- Alumina-Modified Zeolite Recovered from Fly Ash," *J. Hazard. Mater.*, **148**(3), 721-726(2007).
18. Velazquez-Pena, C. G. Solache-Ríos, Olguin, and M. T. and Fall, C., "As(V) Sorption by Different Natural Zeolite Frameworks Modified with Fe, Zr and FeZr," *Microporous and Mesoporous Materials*, **273**, 133-141(2019).
  19. Shi, J., Zhao, Z., Zhou, J. and Liang, Z., "Enhanced Adsorption of As(III) on Chemically Modified Activated Carbon Fibers," *Appl Water Sci.*, **9**, 41(2019).
  20. Banerjee, K., Amy, G. L., Prevost, M., Nour, S., Jekel, M., Gallagher, P. M. and Blumenschein, C. D., "Kinetic and Thermodynamic Aspects of Adsorption of Arsenic onto Granular Ferric Hydroxide (GFH)," *Water Res.*, **42**(13), 3371-3378(2008).
  21. Tan, X. F., Zeng, Y. G., Wang, X., Hu, X., Gu, Y. and Yang, Z., "Application of Biochar for The Removal of Pollutants from Aqueous Solutions," *Chemosphere*, **125**, 70-85(2015).
  22. Thines, K. R., Abdullah, E. C., Mubarak, N. M. and Ruthiraan, M., "Synthesis of Magnetic Biochar from Agricultural Waste Biomass to Enhancing Route for Waste Water and Polymer Application: A Review," *Renewable and Sustainable Energy Reviews*, **67**, 257-76(2017).
  23. Li, H., Dong, X., Silva, E. B., Oliveira, L. M., Chen, Y. and Ma, L. Q., "Mechanisms of Metal Sorption by Biochars," *Chemosphere*, **178**, 466-78(2017).
  24. Zhao, Y., Feng, D., Zhang, Y., Tang, W., Meng, S., Guo, Y. and Sun, S., "Migration of Alkali and Alkaline Earth Metallic Species and Structure Analysis of Sawdust Pyrolysis Biochar," *Korean Chem. Eng. Res.*, **54**(5), 659-664(2016).
  25. Kaushal, I., Maken, S., Sharma, A. K., "SnO<sub>2</sub> Mixed Banana Peel Derived Biochar Composite for Supercapacitor Application," *Korean Chem. Eng. Res.*, **56**(5), 694-704(2018).
  26. Regmi, P., Garcia Moscoso, J. L., Kumar, S., Cao, X., Mao, J. and Schafran, G., "Removal of Copper and Cadmium from Aqueous Solution using Switchgrass Biochar Produced via Hydrothermal Carbonization Process," *J. of Environmental Management*, **109**, 61-9(2012).
  27. Pellerá, F. M., Giannis, A., Kalderis, D., Anastasiadou, K., Stegmann, R., Wang, J. Y. and Gidarakos, E., "Adsorption of Cu(II) Ions from Aqueous Solutions on Biochars Prepared from Agricultural By-products," *J. of Environmental Management*, **96**, 35-42(2012).
  28. Tong, X. J., Li, J. Y., Yuan, J. H. and Xu, R. K., "Adsorption of Cu(II) by Biochars Generated from Three Crop Straws," *Chemical Engineering J.*, **172**, 828-34(2011).
  29. Baig, S. A., Zhu, J., Muhammad, N. and Sheng, X. X., "Effect of Synthesis Methods on Magnetic Kans Grass Biochar for Enhanced As (III,V) Adsorption from Aqueous Solutions," *Biomass and Bioenergy*, **71**, 299-310(2014).
  30. Agrafioti, E., Kalderis, D. and Diamadopoulou, E., "Arsenic and Chromium Removal from Water using Biochars Derived from Rice Husk," *Organic Solid Wastes and Sewage Sludge*, **133**, 309-14(2014).
  31. Wang, S., Gao, B., Zimmermann, A. M., Li, Y., Ma, L., Harris, W. G. and Migliaccio, K. W., "Physicochemical and Sorptive Properties of Biochars Derived from Woody and Herbaceous Biomass," *Chemosphere*, **134**, 257-62(2015).
  32. Zhang, M. and Gao, B., "Removal of Arsenic, Methylene Blue, and Phosphate by Biochar/AlOOH Nanocomposite," *Chemical Engineering J.*, **226**, 286-292(2013).
  33. Li, Y., Mosa, A., Zimmerman, A. R., Ma, L. Q., Harris, W. G. and Migliaccio, K. W., "Manganese Oxide-Modified Biochars: Preparation, Characterization, and Sorption of Arsenate and Lead," *Bioresource Technology*, **181**, 13-17(2015).
  34. Liu, Z., Zhang, F. S. and Sasai, R., "Arsenate Removal from Water Using Fe<sub>3</sub>O<sub>4</sub>-Loaded Activated Carbon Prepared from Waste Biomass," *Chemical Engineering J.*, **160**, 57-62(2010).
  35. Aredes, S., Klein, B. and Pawlik, M., "The Removal of Arsenic from Water Using Natural Iron Oxide Minerals," *J. of Cleaner Production*, **29-30**, 208-13(2012).
  36. Wang, S., Gao, B., Zimmermann, A. M., Li, Y., Ma, L., Harris, W. G. and Migliaccio, K. W., "Removal of Arsenic by Magnetic Biochar Prepared from Pinewood and Natural Hematite," *Bioresource Technology*, **175**, 391-5(2015).
  37. Zhang, M., Gao, B., Varnosfaderani, S., Hebard, A., Yao, Y. and Inyang, M., "Preparation and Characterization of a Novel Magnetic Biochar for Arsenic Removal," *Bioresource Technology*, **130**, 457-62(2013).
  38. Kaygusuz, K. and Sekerci, T., "Biomass for Efficiency and Sustainability Energy Utilization in Turkey," *J. Eng. Res. App. Sci.*, **5**, 332-341(2016).
  39. Ahmad, M., Lee, S. S., Dou, X., Mohan, D., Sung, J. K., Yang, J. E. and Ok, Y. S., "Effects of Pyrolysis Temperature on Soybean Stover and Peanut Shell-Derived Biochar Properties and TCE Adsorption in Water," *Bioresource Technology*, **118**, 536-544(2012).
  40. Agrafioti, E., Kalderis, D. and Diamadopoulou, E., "Ca and Fe Modified Biochars as Adsorbents of Arsenic and Chromium in Aqueous Solutions," *J. of Environmental Management*, **146**, 444-450(2014).
  41. Jin, J. W., Li, Y. A., Zhang, J. Y., Wu, S. C., Cao, Y. C., Liang, P., Zhang, J., Wong, M. H., Wang, M. Y., Shan, S. D. and Christie, P., "Influence of Pyrolysis Temperature on Properties and Environmental Safety of Heavy Metals in Biochars Derived from Municipal Sewage Sludge," *J. of Hazardous Materials*, **320**, 417-426(2016).
  42. Joseph, S. D., Downie, A., Crosky, A., Lehman, J. and Munroe, P., "Biochar for Carbon Sequestration, Reduction of Greenhouse Gas Emissions and Enhancement of Soil Fertility; A Review of the Materials Science. Proceedings of the Australian Combustion Symposium (2007).
  43. Triolo, J. M., Ward, A. J., Pedersen, L. and Sommer, S. G., in Matovic M. D. (Ed.), Characteristics of Animal Slurry as a Key Biomass for Biogas Production in Denmark, Biomass Now-Sustainable Growth and Use, IntechOpen, New York (2013).
  44. Samsuri, A. W., Sadegh-Zadeh, F. and Seh-Bardan, B. J., "Adsorption of As(III) and As(V) by Fe Coated Biochars and Biochars Produced from Empty Fruit Bunch and Rice Husk," *J. of Environmental Chemical Engineering*, **1**, 981-988(2013).
  45. Inyang, M., Gao, B., Zimmerman, A., Zhang, M. and Chen, H., "Synthesis, Characterization, and Dye Sorption Ability of Carbon Nanotube-Biochar Nanocomposites," *Chem. Eng. J.*, **236**, 39-46(2014).
  46. Namduri, H. and Nasrazadani, S., Quantitative Analysis of Iron Oxides Using Fourier Transform Infrared Spectrophotometry,"

- Corros. Sci.*, **50**, 2493-2497(2008).
47. Akyürek, Z., "Sustainable Valorization of Animal Manure and Recycled Polyester: Co-pyrolysis Synergy," *Sustainability*, **11**(8), 2280(2019).
48. Tang, J., Huang, Y., Gong, Y., Lyu, H., Wang, Q. and Ma, J., "Preparation of a Novel Graphen Oxide/Fe-Mn Composite and Its Application for Aqueous Hg(II) Removal," *J. of Hazardous Materials*, **316**, 151-158(2016).
49. Yang, Y., Lin, X., Wei, B., Zhao, Y. and Wang, J., "Evaluation of Adsorption Potential of Bamboo Biochar for Metal-Complex Dye: Equilibrium, Kinetics and Artificial Neural Network Modeling," *Int. J. Environ. Sci. Technol.*, **11**, 1093-1100(2014).
50. He, R., Peng, Z., Lyu H., Huang, H., Nan, Q. and Tang, J., "Synthesis and Characterization of An Iron-Impregnated Biochar for Aqueous Arsenic Removal," *Science of the Total Environment*, **612**, 1177-1186(2018).
51. Vitela-Rodriguez, A. V. and Rangel-Mendez, J. R., "Arsenic Removal by Modified Activated Carbons with Iron Hydro(oxide) Nanoparticles," *J. Environ. Manag.*, **114**, 225-231(2013).
52. Chang, Q., Lin, W. and Ying, W. C., "Preparation of Iron-Impregnated Granular Activated Carbon for Arsenic Removal from Drinking Water," *J. Hazard. Mater.*, **184**, 515-522(2010).
53. Pehlivan, E., Tran, T., Ouédraogo, W., Schmidt, C., Zachmann, D. and Bahadır, M., "Removal of As (V) from Aqueous Solutions by Iron Coated Rice Husk," *Fuel Process. Technol.* **106**, 511-517(2013).
54. Duan, X., Zhang, C., Srinivasakannan, C. and Wang, X., "Waste Walnut Shell Valorization to Iron Loaded Biochar and Its Application to Arsenic Removal," *Resource-Efficient Technologies*, **3**, 29-36(2017).
55. Lata, S., Singh, P. K. and Samadder, S. R., "Regeneration of Adsorbents and Recovery of Heavy Metals: A Review," *Int. J. Environ. Sci. Technol.*, **12**, 1461-78(2015).
56. Wang, S. Tang, Y. Chen, C., Wu, J., Huang, Z., Mo, Y., Zhang, K. and Chen, J., "Regeneration of Magnetic Biochar Derived from Eucalyptus Leaf Residue for Lead(II) Removal," *Bioresource Technol.*, **186**, 360-4(2015).

#### Authors

**Zuhal Akyürek:** Associate Professor, Department of Energy Systems Engineering, Burdur Mehmet Akif Ersoy University, Burdur 15030, Turkey; drzuhalakyurek@gmail.com

**Hande Çelebi:** Associate Professor, Department of Chemical Engineering, Eskişehir Technical University, Eskişehir 26555, Turkey; handed@eskisehir.edu.tr

**Gaye Ö. Çakal:** Associate Professor, Insitute of Nuclear Sciences, Ankara University, Ankara 06560, Turkey; gcakal@ankara.edu.tr

**Sevnur Turgut:** Graduate Student, Department of Materials Sciences Engineering, Burdur Mehmet Akif Ersoy University, Burdur 15030, Turkey; sevnurtuzcu